

# NJC

Accepted Manuscript



This is an *Accepted Manuscript*, which has been through the Royal Society of Chemistry peer review process and has been accepted for publication.

*Accepted Manuscripts* are published online shortly after acceptance, before technical editing, formatting and proof reading. Using this free service, authors can make their results available to the community, in citable form, before we publish the edited article. We will replace this *Accepted Manuscript* with the edited and formatted *Advance Article* as soon as it is available.

You can find more information about *Accepted Manuscripts* in the [Information for Authors](#).

Please note that technical editing may introduce minor changes to the text and/or graphics, which may alter content. The journal's standard [Terms & Conditions](#) and the [Ethical guidelines](#) still apply. In no event shall the Royal Society of Chemistry be held responsible for any errors or omissions in this *Accepted Manuscript* or any consequences arising from the use of any information it contains.

1 **Enhanced Catalytic Performance for Metathesis Reactions over Ordered**

2 **Tungsten and Aluminum Co-doped Mesoporous KIT-6 Catalysts**

3 Huan Liu,<sup>a,b</sup> Kai Tao,<sup>a,\*</sup> Peipei Zhang,<sup>a</sup> Wei Xu,<sup>a</sup> Shenghu Zhou,<sup>a,\*</sup>

4 <sup>a</sup>Ningbo Institute of Materials Technology and Engineering, Chinese Academy of

5 Sciences, Ningbo, Zhejiang 315201, China

6 <sup>b</sup>Shanghai Key Laboratory of Atmospheric Particle Pollution and Prevention (LAP<sup>3</sup>),

7 Department of Environmental Science and Engineering, Fudan University, Shanghai 2

8 00433, China

9

10

11

12

13

14

15

16

17

18

19

20 **\*Corresponding authors**

21 Tel.: (+86) 574 86696927

22 Fax: (+86) 574 86685043

23 E-mail: zhoush@nimte.ac.cn (S. Z.); taokai@nimte.ac.cn (K. T.)

## 1 Abstract

2 Ordered tungsten and aluminum co-doped mesoporous KIT-6 catalysts  
3 (W-Al-KIT-6) with different Si/Al molar ratios were successfully synthesized by a  
4 one-pot synthesis method. The obtained W-Al-KIT-6 catalysts were tested for  
5 catalytic conversion of 1-butene and ethene to propene via isomerization of 1-butene  
6 to 2-butene and subsequent cross metathesis of 2-butene and ethene. Various  
7 characterization techniques, such as ICP-OES, XRD, BET, TEM, Raman, XPS and  
8 NH<sub>3</sub>-TPD, were used to characterize the catalysts. The introduction of Al did not  
9 change the mesoporous structure of KIT-6, when the nominal Si/Al was 10, 20 or 30.  
10 Besides, the sample demonstrated a larger amount of acidic sites. The W-Al-KIT-6  
11 catalysts with suitable Si/Al ratios illustrated a superior catalytic performance to  
12 W-KIT-6 catalyst. The origin of catalytic performance enhancement over  
13 W-Al-KIT-6 catalysts was preliminarily discussed, and ascribed to highly dispersed  
14 W species and a large amount of acidic sites. The acidic sites were formed by  
15 introduction of a suitable amount of Al in the W-KIT-6 framework, which accelerated  
16 the isomerization of 1-butene to 2-butene and promoted the cross metathesis of  
17 2-butene and ethene to propene.

18 **Key Words:** aluminum doping; metathesis; mesoporous; KIT-6; propene

## 19 1. Introduction

20 With the increasing demand of propene, cross-metathesis of butene and ethene to  
21 propene has attracted more and more attentions in recent years.<sup>1</sup> Supported WO<sub>3</sub>  
22 catalysts showing a moderate activity, outstanding stability, anti-poisoning property,

1 as well as low price, were highly desirable for industrial metathesis.<sup>2,3</sup>

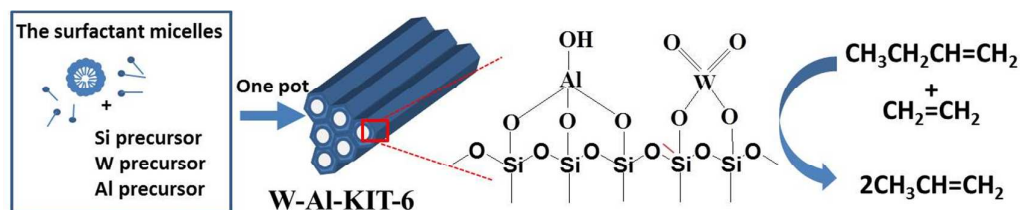
2 The catalytic performance of supported tungsten oxides for olefin metathesis is  
3 determined by many factors, of which the supports have a significant influence on the  
4 physico-chemical properties of catalysts, such as structures and dispersion of tungsten  
5 oxide species, and thus significantly influence the catalytic performance.<sup>4</sup>  
6 Conventional support materials for metathesis catalysts include commercially  
7 available silica gel,  $\gamma$ -Al<sub>2</sub>O<sub>3</sub>,  $\alpha$ -Al<sub>2</sub>O<sub>3</sub>, and mixed oxides such as SiO<sub>2</sub>-Al<sub>2</sub>O<sub>3</sub>,<sup>5</sup> and  
8 zeolite-Al<sub>2</sub>O<sub>3</sub>.<sup>6</sup> Compared with these traditional supports, mesoporous materials show  
9 uniform pores, large BET surface areas and pore volumes, which are beneficial for  
10 dispersion of active species and providing rapid transportation channels for reactants  
11 and products. Thus, great efforts are made to develop highly efficient mesoporous  
12 catalysts for various reactions<sup>7,8</sup> during the last decades. So far, many mesoporous  
13 materials have been explored in olefin metathesis,<sup>9</sup> such as HMS,<sup>10</sup> SBA-15,<sup>11,12</sup>  
14 MCM-41,<sup>13</sup> and FDU-12.<sup>14</sup> Generally, mesoporous catalysts showed much higher  
15 catalytic activity than conventional SiO<sub>2</sub> or Al<sub>2</sub>O<sub>3</sub> supported catalysts due to the high  
16 dispersed active species on the mesoporous supports.

17 On the other hand, it has been demonstrated that the Brønsted acidity of the  
18 supports would be beneficial for olefin metathesis.<sup>6</sup> Literature has revealed that  
19 alumina supported tungsten oxides exhibits strong acid sites and tungsten-support  
20 interaction, but too strong acid sites could induce by-reactions such as cracking and  
21 isomerization.<sup>15</sup> In contrast, silica supported tungsten oxides were barely acidic and  
22 could suppress the by-reactions.<sup>16</sup> However, the weak interaction between W species

1 and silica could result in poor dispersion of tungsten oxide species, causing a poor  
2 catalytic performance. Mixed silica-alumina materials with moderate acidity and  
3 interaction between metal and support are promising as catalyst supports for olefin  
4 metathesis reactions. Xu et al.<sup>6</sup> reported that  $\text{WO}_3/\text{HY-Al}_2\text{O}_3$  catalysts exhibited  
5 higher activity than  $\text{WO}_3/\text{Al}_2\text{O}_3$  with HY content in the range of 0–30 wt%. The  
6 improved catalytic performance over  $\text{WO}_3/\text{HY-Al}_2\text{O}_3$  was ascribed to the moderate  
7 acidity of the supports and the suitable interaction between W species and support.  
8 The same phenomenon was also found in supported Mo or Re catalysts. Literature has  
9 reported that  $\text{MoO}_3/\text{Al}_2\text{O}_3\text{-SiO}_2$  and  $\text{Re}_2\text{O}_7/\text{Al}_2\text{O}_3\text{-SiO}_2$  catalysts were more active  
10 than alumina or silica supported catalysts due to high dispersion of active species and  
11 moderate acidity.<sup>17-19</sup>

12 Here, we first report one-pot synthesis of ordered tungsten and aluminum  
13 co-doped mesoporous KIT-6 materials (W-Al-KIT-6) for metathesis of 1-butene and  
14 ethene to propene. KIT-6, a mesoporous silica with 3D interconnected large  
15 mesopores, has been shown to be an advanced support for many reactions.<sup>20,21</sup> In our  
16 previous work, we successfully synthesized tungsten doped KIT-6 catalysts  
17 (W-KIT-6), and the obtained W-KIT-6 exhibited excellent catalytic performance for  
18 metathesis reactions.<sup>22, 23</sup> In this work, Al and W were co-doped into the KIT-6  
19 framework simultaneously by a one-pot method. The schematic demonstration of  
20 synthesis of tungsten and aluminum co-doped W-Al-KIT-6 is shown in Scheme 1. Al  
21 is introduced to form the acid center and improve the performance of catalysts. The  
22 influence of Si/Al ratio on physico-chemical properties was systematically

1 investigated with various characterization techniques, and the catalytic performance  
 2 for metathesis of 1-butene and ethene to propene over W-Al-KIT-6 with different  
 3 Si/Al ratios was also studied.



4  
 5 **Scheme 1.** The schematic demonstration of synthesis of ordered tungsten and  
 6 aluminum co-doped mesoporous KIT-6 materials.

## 7 2. Experimental section

### 8 2.1. Chemicals

9 Poly (ethylene glycol)-block-poly (propylene glycol)-block-poly (ethylene glycol)  
 10 (P123,  $M_w=5800$ , EO20PO70EO20) was purchased from Aldrich as the structure  
 11 directing agents. Tetraethyl orthosilicate (TEOS, AR) as the silica source was  
 12 purchased from Aladdin. Sodium tungstate dihydrate ( $\text{Na}_2\text{WO}_4 \cdot 2\text{H}_2\text{O}$ , AR),  
 13 hydrochloric acid (HCl, AR), and n-butanol (AR) were purchased from Sinopharm  
 14 Chemical Reagent Co., Ltd.. Aluminum-isopropoxide as the Al source was purchased  
 15 from Chengdu Gray West Chemistry Technology Company. Ammonium  
 16 metatungstate ( $(\text{NH}_4)_6\text{H}_2\text{W}_{12}\text{O}_{40} \cdot x\text{H}_2\text{O}$ ) was obtained from Kunshan Xingbang W&M  
 17 Technology Company. All chemicals were used as received without further  
 18 purification.

### 19 2.2. Catalyst preparation

#### 20 2.2.1 Synthesis of W-KIT-6

1 W-KIT-6 catalysts with a Si/W ratio of 40/1 was prepared according to our  
2 previous study.<sup>22</sup> Typically, 3.0 g of P123 was dissolved in 108.5 g of deionized water,  
3 and 3.0 g of 1-butanol and 5.9 g of HCl (35 wt%) were added into the above solution.  
4 The mixture was vigorously stirred at 35 °C for 1 h and then 6.45 g of TEOS was  
5 slowly added into the solution. After that, the mixture was vigorously stirred at 35 °C  
6 for 1 h, and 0.25 g of sodium tungstate dissolved in 6 mL of water (Si/W=40/1) was  
7 dropwise added into the above solution, and the obtained mixture was further stirred  
8 for another 24 h. The resultant mixture was transferred to a Teflon-lined autoclave and  
9 heated at 100 °C for 24 h. The solid products were collected by filtering, washing  
10 thoroughly with deionized water and drying at 100 °C overnight. Finally, the powders  
11 were calcined in a muffle furnace at 550 °C for 4 h with a heating rate of 1.0 °C/min  
12 to remove P123 surfactants. KIT-6 was also synthesized using the same procedure as  
13 that of W-KIT-6 without adding sodium tungstate.

#### 14 **2.2.2 One-pot synthesis of W-Al-KIT-6**

15 The incorporation of Al in W-KIT-6 was carried out by a one-pot synthesis  
16 method using aluminum-isopropoxide as Al source. In a typical synthesis for  
17 W-Al-KIT-6 with a Si/Al ratio of 10/1, 0.63 g of aluminum-isopropoxide were  
18 dissolved in a solution containing 108.5 g of deionized water and 5.9 g of HCl (35  
19 wt%). The solution was vigorously stirred at 35 °C for at least 1 h, and then 3.0 g of  
20 P123 and 3.0 g of 1-butanol were added into the above solution. The mixture was  
21 vigorously stirred at 35 °C for 1 h, and then 6.45 g of TEOS (Si/Al=10/1) was slowly  
22 added into the solution. After that, the mixture was vigorously stirred at 35 °C for 1 h.

1 A solution containing 0.25 g of sodium tungstate dihydrate and 6 mL of water  
2 (Si/W=40) was dropwise added into the above solution, and the resultant mixture was  
3 stirred for another 24 h. W-Al-KIT-6 was obtained after the same hydrothermal  
4 treatment, collecting procedures and calcination process as those of W-KIT-6. The  
5 W-Al-KIT-6 with other Si/Al ratios were synthesized by the same procedures except  
6 that the amount of aluminum-isopropoxide was changed according to the desired  
7 nominal Si/Al ratios. The W-Al-KIT-6 materials with Si/Al ratios of 1/1, 10/1, 20/1  
8 and 30/1 were denoted as W-Al-KIT-6-1, W-Al-KIT-6-10, W-Al-KIT-6-20 and  
9 W-Al-KIT-6-30, respectively.

#### 10 **2.2.3 Preparation of control $WO_3/SiO_2$ catalyst**

11 A control  $WO_3/SiO_2$  catalyst was prepared by impregnating a commercial silica gel  
12 (BET surface area: 399.0 m<sup>2</sup>/g, Qingdao Haiyang Chemical Co. Ltd.) with an aqueous  
13 solution of ammonium metatungstate. The impregnated sample was dried at 100 °C  
14 overnight and subjected to an identical calcination procedure to W-KIT-6 catalyst. The  
15 loading of W was fixed identical to that of W-KIT-6.

#### 16 **2.3. Catalyst characterization.**

17 Elements analysis was conducted by inductively coupled plasma-optical  
18 emission spectroscopy (ICP-OES) using Perkin-Elmer OPTIMA 2100 DV optical  
19 emission spectrometer. Brunauer–Emmett–Teller (BET) surface area, pore volume,  
20 and pore size was obtained using a Micromeritics ASAP 2020M adsorption apparatus.  
21 Prior to measurement, the sample was degassed under vacuum at 200 °C for 3 h.  
22 Small angle and wide angle X-ray diffraction patterns (XRD) were recorded on a

1 Bruker D8 Advance X-Ray diffractometer using Cu K $\alpha$  radiation. Raman spectra  
2 were obtained using a Renishaw Raman spectrometer equipped with a microscope  
3 (laser wavelength of 532 nm). Transmission electron microscopy (TEM) image was  
4 obtained on a JEOL 2100 transmission electron microscope operated at 200kV. The  
5 sample was dispersed in ethanol by sonication and dropped onto a carbon-coated  
6 copper grid followed by evaporating naturally. X-ray photoelectron spectroscopy  
7 (XPS) experiments were performed on an AXIS ULTRA DLD multifunctional X-ray  
8 photoelectron spectroscopy with an Al source. Temperature-programmed desorption  
9 of ammonia (NH<sub>3</sub>-TPD) was carried out in a quartz microreactor. The as-prepared  
10 sample (50.0 mg) was pretreated in N<sub>2</sub> at 600 °C for 0.5 h prior to NH<sub>3</sub>-TPD  
11 measurement, and then a stream of 10/90 (v/v) NH<sub>3</sub>/N<sub>2</sub> was introduced for adsorption  
12 at room temperatures for 0.5 h. The sample was further purged by N<sub>2</sub> for 2 h to  
13 remove the physically absorbed NH<sub>3</sub>. Temperature-programmed desorption of  
14 ammonia was carried out from 50 °C to 800 °C with a ramping rate of 10 °C/min, and  
15 the amount of desorbed NH<sub>3</sub> was monitored by a thermal conductivity detector  
16 (TCD).

#### 17 **2.4 Catalytic conversion of 1-butene and ethene to propene**

18 Catalytic conversion of 1-butene and ethene to propene was carried out in a  
19 fixed-bed stainless steel microreactor (i.d. 10 mm). In each run, 1.0 g of catalyst  
20 (20-40 mesh) was placed in the center of reactor, and the catalyst layer was below and  
21 upper supported by an inert SiO<sub>2</sub> bead layer. The catalysts were pretreated by pure N<sub>2</sub>  
22 at 550 °C for 4 hours (0.1 MPa, 30 mL/min). After cooling down to the reaction

1 temperatures, C<sub>2</sub>H<sub>4</sub> and 1-C<sub>4</sub>H<sub>8</sub> (98 %, Dalian special gas company) were directly  
 2 delivered to the reactor from cylinders. The gas flow rates of C<sub>2</sub>H<sub>4</sub> and 1-C<sub>4</sub>H<sub>8</sub> were  
 3 controlled to by two mass flow controllers (MFC) to keep the molar ratio of  
 4 C<sub>2</sub>H<sub>4</sub>/1-C<sub>4</sub>H<sub>8</sub> equal to 2/1. The metathesis reactions were carried out at ambient  
 5 pressure, reaction temperature from 400 to 500 °C, and gas hourly space velocity  
 6 (WHSV) of 0.8 h<sup>-1</sup>. All products were analyzed online using a gas chromatograph  
 7 equipped with a flame ionization detector (FID). The 1-butene conversion and product  
 8 selectivity were calculated by following formulas:

$$9 \quad x_{1-butene} = \frac{[C_3^-]_n + 2[2-C_4^-]_n}{[C_3^-]_n + 2[1-C_4^-]_n + 2[2-C_4^-]_n + 2[iso-C_4^-]_n} \quad (1)$$

$$10 \quad S_{propene} = \frac{[C_3^-]_m}{[C_3^-]_m + [2-C_4^-]_m + [iso-C_4^-]_m} \quad (2)$$

$$11 \quad S_{2-butene} = \frac{[2-C_4^-]_m}{[C_3^-]_m + [2-C_4^-]_m + [iso-C_4^-]_m} \quad (3)$$

12 Where [C<sub>3</sub><sup>-</sup>]<sub>n</sub>, [1-C<sub>4</sub><sup>-</sup>]<sub>n</sub>, [2-C<sub>4</sub><sup>-</sup>]<sub>n</sub> and [iso-C<sub>4</sub><sup>-</sup>]<sub>n</sub> are the molar fraction of each  
 13 component in effluent gas, and [C<sub>3</sub><sup>-</sup>]<sub>m</sub>, [1-C<sub>4</sub><sup>-</sup>]<sub>m</sub>, and [iso-C<sub>4</sub><sup>-</sup>]<sub>m</sub> are the mass fraction  
 14 of each component in effluent gas.

### 15 **3. Results and discussion**

#### 16 **3.1 Characterization of catalysts**

##### 17 **3.1.1 Elemental analysis**

18 ICP-OES analysis is performed to determine the real content of Na, W and Al in  
 19 the final products. The result suggested that only trace amount of Na (below 0.1 wt %)  
 20 was left in the catalyst, since the sample was washed thoroughly before calcination.  
 21 Table 1 summarized the real loading of W and Al in final catalysts. Approximately

1 67-80 % of W species in the initial synthesis gel was introduced in the final  
 2 W-Al-KIT-6, and this tendency was consistent with literature.<sup>22</sup> In contrast,  
 3 approximately 21 % of Al species in the initial synthesis gel was introduced in the  
 4 final W-Al-KIT-6 at the Si/Al ratios ranging from 10/1 to 30/1 while ~40 % of Al  
 5 species in the initial synthesis gel was introduced in the final products at the Si/Al  
 6 ratio of 1/1. A limited amount of Al doped in the final product was also reported by  
 7 literatures.<sup>24,25</sup> In the acidic medium, most of Al species were in cationic forms rather  
 8 than oxo forms (necessary for formation of Si–O–Al linkages), restricting the amount  
 9 of Al species in the final products.

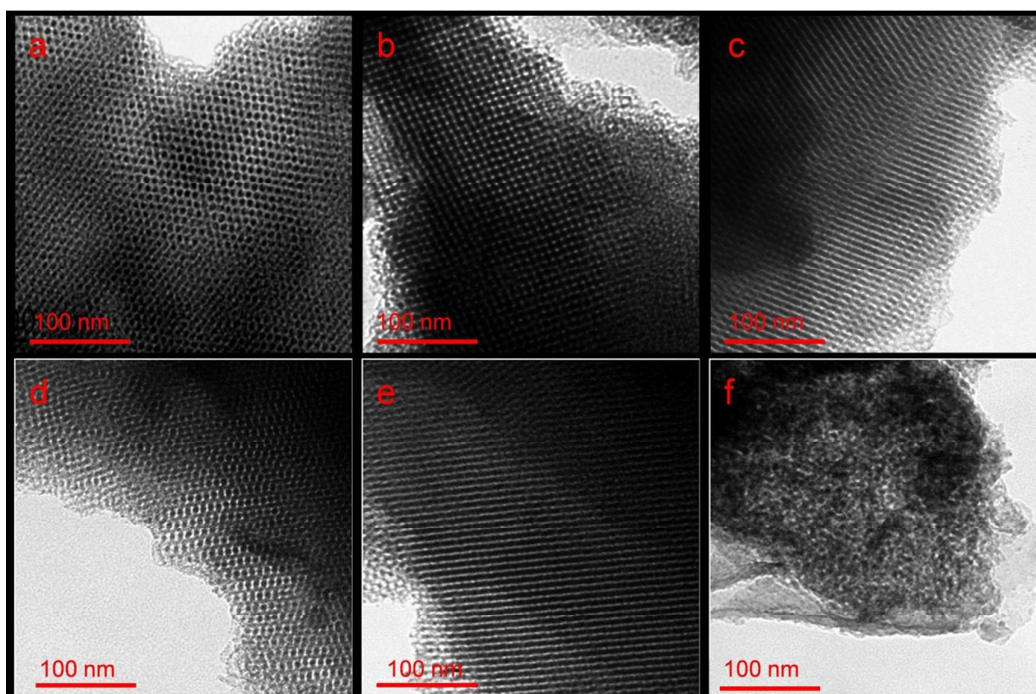
10 **Table 1.** Elemental analysis of various catalysts by ICP-OES.

Catalysts	Si/W (molar)		Si/Al (molar)		Product	
	Gel	Product	Gel	Product	W (wt %)	Al (wt %)
KIT-6	N/A	N/A	N/A	N/A	N/A	N/A
WO <sub>3</sub> /SiO <sub>2</sub>	40/1	N/A	N/A	N/A	4.85	N/A
W-KIT-6	40/1	58/1	N/A	N/A	5.01	N/A
W-Al-KIT-6-30	40/1	55/1	30/1	138/1	5.26	0.30
W-Al-KIT-6-20	40/1	51/1	20/1	94/1	5.51	0.44
W-Al-KIT-6-10	40/1	53/1	10/1	47/1	5.06	0.88
W-Al-KIT-6-1	40/1	59/1	1/1	2.5/1	3.49	12.93

11 **3.1.2 Transmission electron microscope**

12 TEM images of various samples are illustrated in Figure 1. As shown in Figure  
 13 1a, KIT-6 exhibited a three dimensional (3D) ordered mesoporous structure, which

1 was consistent with literatures.<sup>26,27</sup> The W doped KIT-6 samples (W-KIT-6) in Figure  
2 1b also showed a well-ordered mesoporous structure, except for few irregular  
3 domains at the peripheries of the materials. The introduction of Al did not change the  
4 structure/texture/appearance of the sample (when Si/Al in 10, 20 or 30) as shown in  
5 Figure 1c, d and e. However, for the W-Al-KIT-6-1 (Figure 1f) at the highest ratio of  
6 Al/Si, the ordered mesoporous structures disappeared, showing disordered structures.  
7 It is suggested that the introduction of a proper amount of Al is beneficial for  
8 maintenance of mesoporous structures and excess Al introduction cause the collapse  
9 of mesoporous structure.

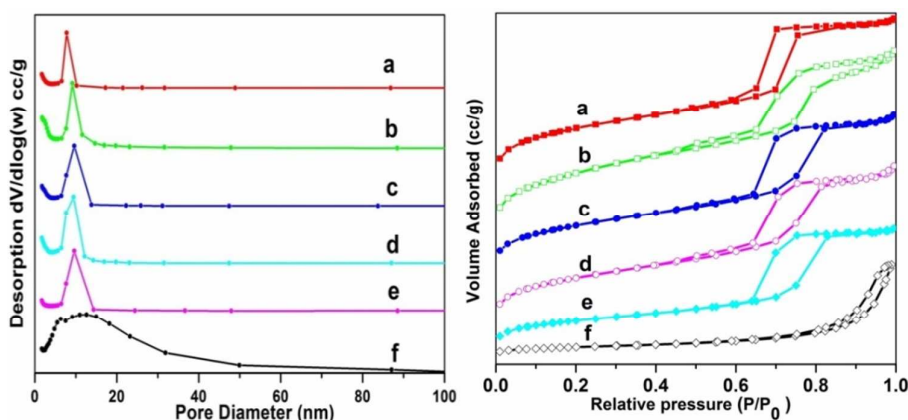


10  
11 **Figure 1.** TEM images showing a), KIT-6; b), W-KIT-6; c), W-Al-KIT-6-30; d),  
12 W-Al-KIT-6-20; e), W-Al-KIT-6-10; f), W-Al-KIT-6-1. Scale bars are 100 nm.

### 13 *3.1.3 Nitrogen physisorption*

14 The N<sub>2</sub> adsorption isotherms and BJH pore size distributions of KIT-6, W-KIT-6

1 and W-Al-KIT-6 materials are shown in Figure 2. Except for W-Al-KIT-6-1, all  
 2 samples showed type IV isotherms with H1 hysteresis loops, which revealed that all  
 3 samples had ordered mesoporous channels.<sup>28</sup> The sharp capillary condensation feature  
 4 at relative pressure of 0.6-0.8 ( $P/P_0$ ) indicating the existence of uniform pores in all  
 5 samples. It is clearly observed that all samples except W-Al-KIT-6-1 show narrow  
 6 pore-size distributions. An increase of the Si/Al ratio typically resulted in a small  
 7 increase in the average pore size, so the pore diameter showed a slight shift. For  
 8 W-Al-KIT-6-1, the isotherm and pore size distribution was significantly different from  
 9 that of W-KIT-6 and W-Al-KIT-6 catalyst with Si/Al of 10, 20 or 30. It is indicated  
 10 that the ordered mesoporous structure of KIT-6 is disappeared as confirmed by TEM  
 11 observation (Figure 1f).



12  
 13 **Figure 2.** N<sub>2</sub> adsorption–desorption isotherms (left panel) and pore size distributions  
 14 (right panel) showing a), KIT-6; b), W-KIT-6; c), W-Al-KIT-6-30; d), W-Al-KIT-6-20;  
 15 e), W-Al-KIT-6-10 and f), W-Al-KIT-6-1.

16 Table 2 summarizes the BET surface areas, pore volumes and mean pore sizes of  
 17 different samples. The reduction of BET surface areas and pore volumes are observed  
 18 for W-KIT-6, as compared with these of KIT-6. However, after the introduction of an

1 appropriate amount of Al, W-Al-KIT-6-30, W-Al-KIT-6-20 or W-Al-KIT-6-10 showed  
 2 slightly improved BET surface area, pore volume and pore size as compared with that  
 3 of W-KIT-6, which suggested that the incorporation of a suitable amount of Al did not  
 4 disturb the mesoporous structure. In contrast, the W-Al-KIT-6-1 sample with the  
 5 highest Al/Si ratio exhibited a drastic reduction of BET surface areas due to the  
 6 collapse of mesoporous structures and blocking of pores caused by excess aluminum.

7 **Table 2.** BET surface areas, pore volumes, and pore sizes of various catalysts.

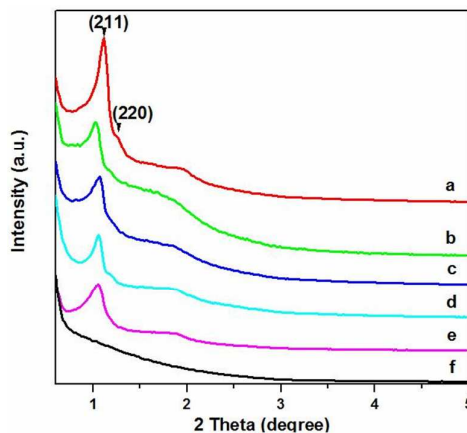
Catalysts	$a_0^a$ (nm)	BET surface area (m <sup>2</sup> /g)	Pore volume (cm <sup>3</sup> /g)	Average pore size (nm)	Acidity amount ( $\mu$ mol/g)
KIT-6	19.6	835	0.98	4.6	68.1
W-KIT-6	21.0	721	0.81	4.6	126.3
W-Al-KIT-6-30	20.6	764	0.93	5.1	191.6
W-Al-KIT-6-20	20.6	758	0.94	5.1	207.6
W-Al-KIT-6-10	20.8	754	1.1	6.2	232.8
W-Al-KIT-6-1	N/A	265	1.0	15.7	274.6

<sup>a</sup> Unit cell parameter calculated from the formula  $a_0 = 6^{1/2}d_{211}$

### 8 **3.1.4 X-ray diffraction**

9 Small angle XRD measurement is used to study the mesoporosity of various  
 10 samples, and the results are presented in Figure 3. A well-resolved diffraction peak in  
 11 the 1.0-1.1° range was observed for KIT-6, which could be indexed as the (211)  
 12 reflection in the bicontinuous cubic Ia3d symmetry reported for KIT-6.<sup>29</sup> Besides, the  
 13 existence of a broad shoulder corresponding to (220) reflection further indicated

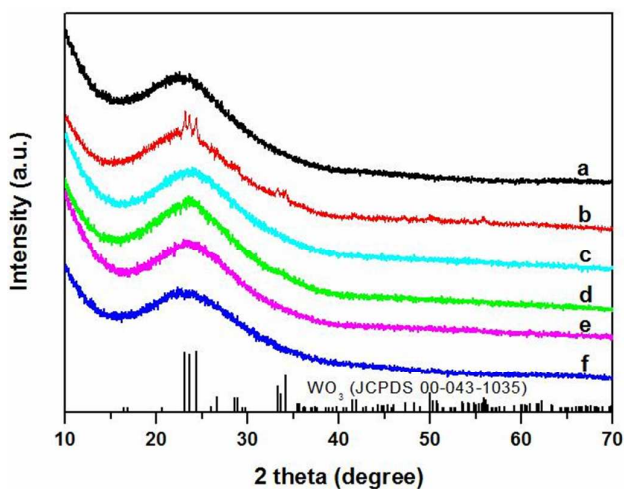
1 ordered mesoporous structures. Except for the W-Al-KIT-6-1 sample at the highest  
2 ratio of Al/Si (Figure 3f), all samples exhibited the well resolved diffraction patterns  
3 similar to KIT-6, confirming that the ordered mesoporous structure of KIT-6 was  
4 maintained after the incorporation of W and Al with suitable Si/Al ratios (10/1, 20/1  
5 or 30/1). For W-Al-KIT-6-1, the absence of diffraction peaks in small angles  
6 suggested the collapse of mesoporous structures. In addition, cubic unit cell  
7 parameters ( $a_0$ ) of samples are also calculated and presented in Table 2. It is found  
8 that the unit cell parameter  $a_0$  increased after introducing of W and Al atoms in the  
9 framework of KIT-6, accompanied by the shift of (211) reflections to lower angles in  
10 Figure 3. This phenomenon may be caused by the doping of tungsten with larger  
11 atomic radius compared to that of  $\text{Si}^{4+}$ .<sup>30, 31</sup>



12  
13 **Figure 3.** Small-angle XRD patterns of various samples showing a), KIT-6; b),  
14 W-KIT-6; c), W-Al-KIT-6-30; d), W-Al-KIT-6-20; e), W-Al-KIT-6-10; f),  
15 W-Al-KIT-6-1.

16 Wide-angle XRD profiles of various samples are shown in Figure 4. KIT-6  
17 showed a broad peak in the  $2\theta$  range from 15 to 30 °C, which are the characteristic

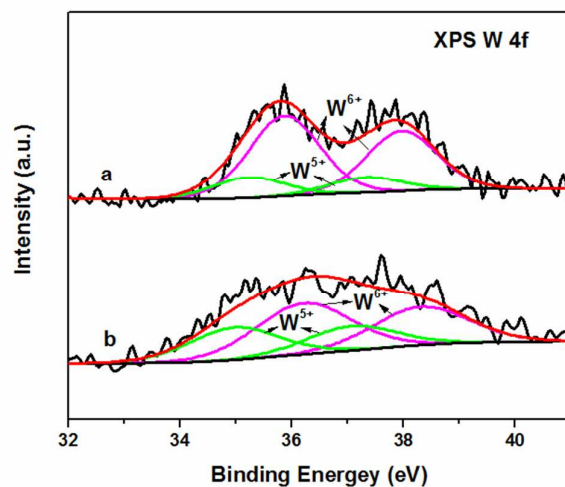
1 diffractions of amorphous silica. Obvious crystalline  $\text{WO}_3$  diffractions (JCPDS  
2 00-043-1035) are observed for W-KIT-6 in Figure 4b, which is due to the formation of  
3  $\text{WO}_3$  extraframework at a high W loading.<sup>22</sup> In contrast, no  $\text{WO}_3$  diffractions are  
4 observed for all W-Al-KIT-6 samples (Figure 4c-f), indicating that the W species are  
5 highly dispersed in W-Al-KIT-6 samples. It is concluded that the introduction of Al in  
6 W-KIT-6 by the current one-pot synthesis method could enhance the dispersion of W  
7 species, which may further enhance the catalytic performance for metathesis of  
8 1-butene and ethene to propene.



9  
10 **Figure 4.** Wide-angle XRD patterns of various samples showing a), KIT-6; b),  
11 W-KIT-6; c), W-Al-KIT-6-30; d), W-Al-KIT-6-20; e), W-Al-KIT-6-10; f),  
12 W-Al-KIT-6-1. Vertical lines indicating the diffractions of crystalline  $\text{WO}_3$  (JCPDS  
13 00-043-1035).

14

### 15 3.1.5 X-ray photoelectron spectroscopy

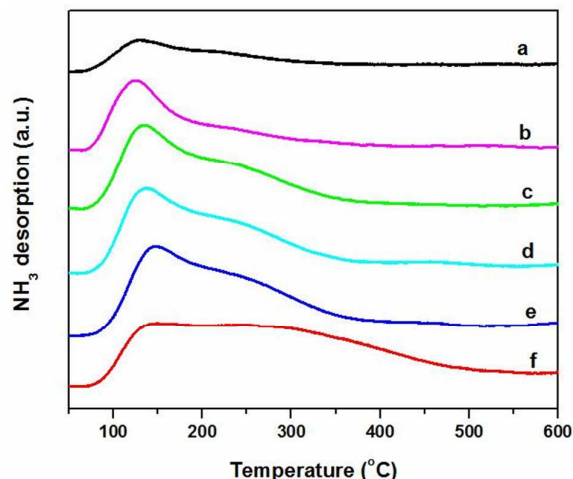


1

2 **Figure 5.** XPS spectra showing a), W-KIT-6; and b), W-Al-KIT-6-10.

3 XPS experiments were carried out to investigate the effect of Al doping on the  
4 oxidation states of tungsten. Figure 5 shows the XPS spectra of the W-KIT-6 and  
5 W-Al-KIT-6-10 samples. The XPS curves were fitted according to the theory of  
6 Doniach and Sunjic.<sup>32</sup> The binding energies of 35.9-36.2 eV and 38.0-38.3 eV were  
7 attributed to 4f<sub>7/2</sub> and 4f<sub>5/2</sub> of W<sup>6+</sup> species while the binding energies of 37.0-37.3 and  
8 34.9-35.2 eV were assigned to 4f<sub>5/2</sub> and 4f<sub>7/2</sub> of W<sup>5+</sup> species.<sup>33-35</sup> The presence of W<sup>5+</sup>  
9 species in W-KIT-6 sample was consistent with our previous work.<sup>22</sup> W<sup>5+</sup> species was  
10 also observed in the W-Al-KIT-6 sample. Table S1 summarizes the molar percentage  
11 of W<sup>6+</sup> and W<sup>5+</sup> species in W-KIT-6 and W-Al-KIT-6-10 samples. The molar  
12 percentage of W<sup>5+</sup> species in W-KIT-6 was 20.6 % while the molar percentage of W<sup>5+</sup>  
13 in W-Al-KIT-6-10 samples increased to 37.5 %. The presence of high concentration of  
14 W<sup>5+</sup> species could favor olefin metathesis, as suggested by the previous studies.<sup>6, 22</sup>

15 **3.1.6 NH<sub>3</sub>-Temperature programmed desorption**



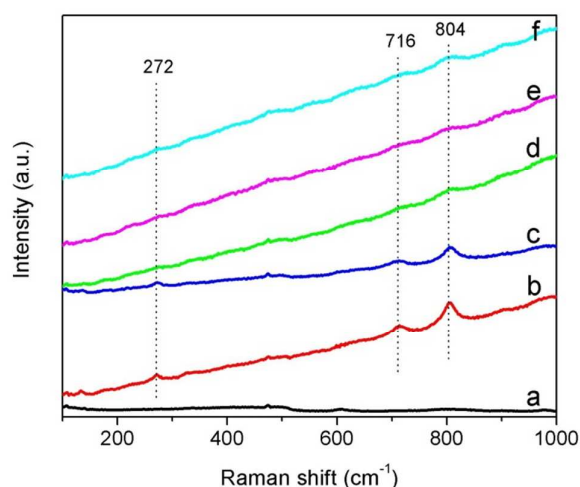
1  
 2 **Figure 6.** NH<sub>3</sub>-TPD profiles of different samples showing a), KIT-6; b), W-KIT-6; c),  
 3 W-Al-KIT-6-30; d), W-Al-KIT-6-20; e), W-Al-KIT-6-10; and f), W-Al-KIT-6-1.

4 NH<sub>3</sub>-TPD technique is used to study the effect of aluminum doping on the  
 5 acidity of catalysts, and the results are shown in Figure 6. KIT-6 showed a weak  
 6 desorption peak centered at 130 °C. In contrast, the W-KIT-6 exhibited an intense  
 7 desorption peak at 125 °C, indicating more acid sites in W doped KIT-6 materials. For  
 8 W-Al-KIT-6 catalysts at the Si/Al ratios of 30/1, 20/1 and 10/1, the main ammonia  
 9 desorption peaks around 130-148 °C with a broad shoulder in the range of 200-500 °C  
 10 range were observed, corresponding to weak and medium acid sites, respectively.<sup>13,36</sup>  
 11 Moreover, with the aluminum content increasing, the ammonia desorption peaks  
 12 became more intense and the peaks shifted to higher temperature range, revealing that  
 13 the total amount of acid sites and the strength of acid increased with the aluminum  
 14 content increasing. Especially for W-Al-KIT-6-1, the NH<sub>3</sub>-TPD profiles showed a  
 15 drastic increase of peak intensity over the 350-500 °C, indicating the drastic increase  
 16 of medium acid sites amount under the same acid strength. The total acidity is  
 17 calculated based on desorbed NH<sub>3</sub> from 50 to 550 °C after steady adsorption and the

1 data are presented in Table 2. Among these materials, the total amount of the acid sites  
2 increased in the following sequence:  
3 KIT-6<W-KIT-6<W-Al-KIT-6-30<W-Al-KIT-6-20<W-Al-KIT-6-10<W-Al-KIT-6-1.

#### 4 **3.1.7 Raman spectra**

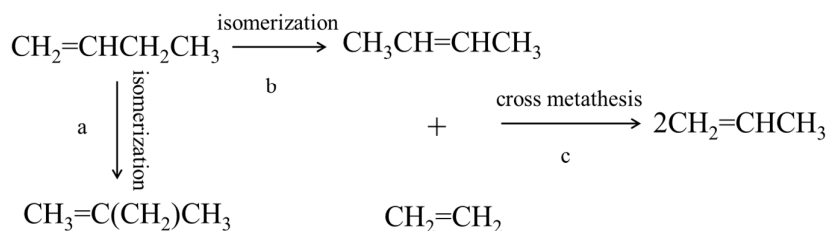
5 Raman spectra of various samples are shown in Figure 6. Three peaks at 804,  
6 716 and 272  $\text{cm}^{-1}$  were observed for W-KIT-6 and for W-Al-KIT-6-30, assigning to  
7 symmetric stretching mode of W-O, bending mode of W-O, and deformation mode of  
8 W-O-W in the crystalline  $\text{WO}_3$ ,<sup>37, 38</sup> respectively. Compared with W-KIT-6,  
9 W-Al-KIT-6-30 showed broader Raman bands, suggesting that the dispersion of W  
10 species in W-Al-KIT-6-30 were better than that of W-KIT-6. With further increasing  
11 the aluminum contents, the W-Al-KIT-6 samples showed very weak Raman peaks of  
12 crystalline  $\text{WO}_3$ , strongly suggesting that the introduction of Al could enhance the  
13 dispersion of W species in the W-Al-KIT-6.



14  
15 **Figure 7.** Raman spectra of different samples showing a), KIT-6; b), W-KIT-6; c),  
16 W-Al-KIT-6-30; d), W-Al-KIT-6-20; e), W-Al-KIT-6-10; f), W-Al-KIT-6-1.

#### 17 **3.2 Catalytic conversion of 1-butene and ethene to propene**

### 1 3.2.1 Effects of mesoporosity and Si/Al ratio



2

3 **Scheme 2.** The main reaction pathways of catalytic conversion of ethene and  
4 1-butene.

5  $\text{WO}_3/\text{SiO}_2$ , W-KIT-6 and W-Al-KIT-6 catalysts are evaluated in catalytic conversion  
6 of 1-butene and ethene to propene. Possible reaction pathways are shown in Scheme 2.  
7 According to the well-established mechanism<sup>39, 40</sup> of olefin metathesis, propene was  
8 mainly produced by the cross metathesis of 2-butene and ethene (Scheme 2a).  
9 Therefore, 1-butene was needed to be first isomerized to 2-butene during the reaction  
10 (Scheme 2b). In our previous work<sup>22</sup> MgO was used as isomerization catalysts and the  
11 catalytic reactions were conducted at 350 °C. In this work, no MgO was added, and  
12 consequently the reactions were carried out at relative higher temperatures in the  
13 range from 400 to 500 °C.

14 The catalytic performances of  $\text{WO}_3/\text{SiO}_2$ , W-KIT-6 and W-Al-KIT-6 catalysts are  
15 compared in Figure 8 and the detailed data are summarized in Table 4.  $\text{WO}_3/\text{SiO}_2$   
16 showed a low 1-butene conversion of 36.6% and propene selectivity of 11.0%. For  
17 mesoporous W-KIT-6, the conversion of 1-butene and selectivity of propene were  
18 55.1 % and 67.1 %, respectively, which were much better than these of conventional  
19 non-mesoporous  $\text{WO}_3/\text{SiO}_2$  catalyst as expected. The incorporation of a suitable  
20 amount of Al into W-KIT-6 resulted in an increase of 1-butene conversion and

propene selectivity. When the Al/Si ratios increased from 1/30 to 1/10, the 1-butene conversion/propene selectivity increased from 59.5 %/68.8 % to 78.2 %/82.4 %, respectively. Moreover, at the range of Al/Si ratios from 1/30 to 1/10, the catalytic performance over W-Al-KIT-6 was quite stable. When introduction of an excess amount of Al into W-KIT-6, the 1-butene conversions and propene selectivity over W-Al-KIT-6-1 decreased, and the catalysts deactivated quickly during the first four hours of reactions.

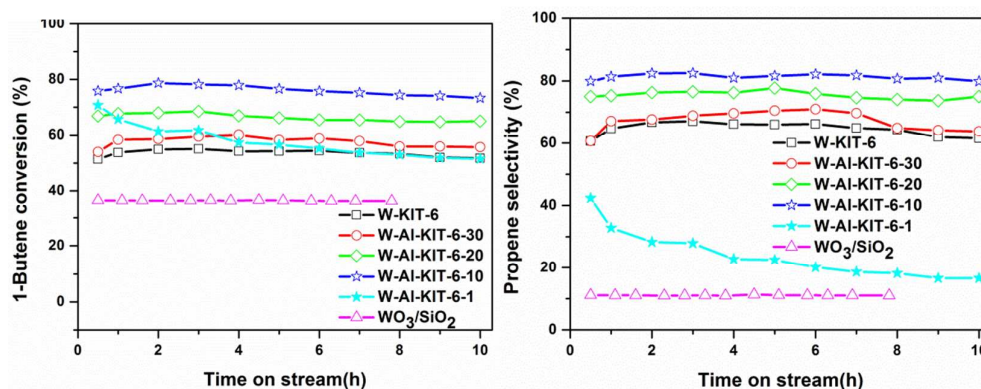


**Figure 8.** 1-butene conversion (left panel) and propene selectivity (right panel) of various catalysts. Reaction conditions: catalyst weight-1.0 g; T=450 °C; P=0.1 MPa; WHSV=0.8 h<sup>-1</sup>; C<sub>2</sub>H<sub>4</sub>/1-C<sub>4</sub>H<sub>8</sub>=2.

It was suggested that highly dispersed surface tetrahedral tungsten species were active while bulk WO<sub>3</sub> were non-active for olefin metathesis.<sup>2</sup> Besides, the acidity of the support was also beneficial for olefin metathesis.<sup>6</sup> In the present work, W-KIT-6 showed a mediate catalytic performance. The doping of an appropriate amount of Al led to an increased amount of acid sites without changing the mesoporous structure of KIT-6 for W-Al-KIT-6 samples (Si/Al=30/1, 20/1 and 10/1), resulting in enhanced catalytic performances. However, for W-Al-KIT-6-1 at the highest Al/Si

1 ratio of 1/1, the collapse of mesoporous structures and an excess amount of acid sites  
 2 induced by the introduction of an excess amount of Al into the framework resulted in  
 3 a poor catalytic performance for metathesis of 1-butene and ethene to propene. As  
 4 shown in Table 3, the high acidity of W-Al-KIT-6-1 caused severe by-reactions, as  
 5 evidenced by 34.1 % of selectivity of isobutene. The high acidity would induce  
 6 1-butene skeletal isomerization to isobutene, as reported in literature (Scheme 2a).<sup>41</sup>

7 **Table 3.** Effect of Si/Al ratios on conversion of 1-butene and product selectivity over  
 8 W-KIT-6 and various W-Al-KIT-6 catalysts.

Catalysts	1-butene conversion (%)	Selectivity (%)		
		Propene	2-butene	Isobutene
WO <sub>3</sub> /SiO <sub>2</sub>	36.6	89.0	11.0	0.0
W-KIT-6	55.1	67.1	32.9	0.0
W-Al-KIT-6-30	59.5	68.8	29.4	1.8
W-Al-KIT-6-20	68.5	76.6	21.0	2.4
W-Al-KIT-6-10	78.2	82.4	12.4	5.2
W-Al-KIT-6-1	61.6	27.9	38.0	34.1

Reaction conditions: catalyst weight-1.0 g; temperature-450 °C; pressure-0.1 MPa;  
 WHSV=0.8 h<sup>-1</sup>; C<sub>2</sub>H<sub>4</sub>/1-C<sub>4</sub>H<sub>8</sub>=2/1; data collected after 3.0 hours of reactions.

9 It is indicated that the amount of Al plays a crucial role in catalytic conversion of  
 10 1-butene and ethene. At higher Si/Al ratio, the W-Al-KIT-6 (Si/Al ratio of 10, 20 or  
 11 30) showed ordered mesoporous structure with moderate acidity. The moderate  
 12 acidity could promote the conversion of 1-butene to 2-butene, and consequently the

1 catalyst showed higher 1-butene conversion and propene selectivity. At low Si/Al  
 2 ratio, the W-Al-KIT-6-1 catalyst exhibited high acidity and deteriorated structure. The  
 3 poor texture resulted in low 1-butene conversion and the high acidity stimulated the  
 4 unwanted side-reaction such as, isomerization or oligomerization reactions, resulting  
 5 low propene selectivity and bad stability. W-Al-KIT-6-10 catalyst with optimum  
 6 amount of Al showed best catalytic performance due to the highly dispersed W  
 7 species and suitable acidity.

### 8 **3.2.1 Effects of reaction temperature**

9 **Table 4.** Effect of reaction temperatures on catalytic performance over  
 10 W-Al-KIT-6-10.

Temperature (°C)	1-butene conversion (%)	Selectivity (%)		
		Propene	2-butene	Isobutene
400	44.3	37.5	58.0	4.5
450	78.2	82.4	12.4	5.2
500	83.5	86.1	9.0	4.9

Reaction conditions: catalyst weight-1.0 g (W-Al-KIT-6-10); pressure-0.1 MPa;  
 WHSV=0.8 h<sup>-1</sup>; C<sub>2</sub>H<sub>4</sub>/1-C<sub>4</sub>H<sub>8</sub>=2/1

11 The influence of reaction temperatures on catalytic performance of W-Al-KIT-6-10  
 12 catalysts was summarized in Table 4. At 400 °C, the catalyst showed 44.4 % of  
 13 1-butene conversion and 37.5 % of propene selectivity. When the reaction temperature  
 14 increased to 450 °C, the 1-butene conversion and propene selectivity increased  
 15 dramatically. Further increasing the temperature resulted in slightly improved

1 catalytic performance.

2 To investigate the stability of catalyst, a longer time on stream reaction over  
3 W-Al-KIT-6-10 catalyst is conducted and the result is presented in Figure S1. The  
4 catalyst showed slight loss of activity after 24 h of reaction. The morphology of spent  
5 catalyst is observed by TEM. The TEM image (Figure S2) of post-reaction  
6 W-Al-KIT-6-10 catalyst suggested that mesoporous structure was well retained  
7 although some domains became non-ordered. The result indicated that the catalyst  
8 showed good stability.

#### 9 **4. Conclusions**

10 Ordered tungsten and aluminum co-doped mesoporous KIT-6 materials were  
11 successfully synthesized by a one-pot method, and their catalytic performances for  
12 catalytic conversion of 1-butene and ethene to propene were investigated.  
13 Characterization results revealed that the doping of an appropriate amount of Al in  
14 W-KIT-6 did not change the mesoporous structure. Besides, the incorporation of Al  
15 could increase the amount of acid sites and favor the dispersion of W species. When  
16 Al/Si ratios ranged from 1/30 to 1/10, W-Al-KIT-6 catalysts showed enhanced  
17 catalytic performance. The introduction of excessive Al resulted in the collapse of  
18 mesoporous structures of KIT-6 and a poor catalytic performance. The improvement  
19 of catalytic activity was ascribed to the retained mesoporous structure, the increased  
20 amount of acid sites and the better dispersion of W species facilitated by Al  
21 incorporation. The introduction of excess Al resulted in collapse of mesoporous  
22 structure and poor catalytic performance. The findings in this study are helpful to

1 design more efficient metathesis catalysts for propene production, and could be  
2 extended to other olefin metathesis reactions.

### 3 Acknowledgments

4 S. Zhou thanks the financial supports from the Ministry of Science and Technology  
5 of China (Grant No. 2012DFA40550) and the aided program for science and  
6 technology innovative research team of Ningbo municipality (2014B81004). K. Tao  
7 thanks the financial support from National Natural Science Foundation of China  
8 (Grant No.51302278) and Natural Science Foundation of Ningbo (Grant No.  
9 2015A610052).

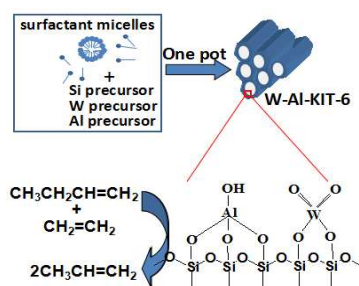
### 10 Reference

- 11 1. J. C. Mol, *J. Mol. Catal. A.*, 2004, **213**, 39-45.
- 12 2. Q. Zhao, S.-L. Chen, J. Gao and C. Xu, *Transition Met. Chem.*, 2009, **34**, 621-627.
- 13 3. A. Spamer, T. I. Dube, D. J. Moodley, C. van Schalkwyk and J. M. Botha, *Appl. Catal., A* 2003, **255**,  
14 133-142.
- 15 4. N. Liu, S. Ding, Y. Cui, N. Xue, L. Peng, X. Guo and W. Ding, *Chem. Eng. Res. Des.*, 2013, 91,  
16 573-580.
- 17 5. M. Sibeijn and J. C. Mol, *Appl. Catal.*, 1990, **67**, 279-295.
- 18 6. S. Huang, S. Liu, W. Xin, J. Bai, S. Xie, Q. Wang and L. Xu, *J. Mol. Catal. A.*, 2005, **226**, 61-68.
- 19 7. L. Zhang, L. Shi, L. Huang, J. Zhang, R. Gao and D. Zhang, *ACS Catal.*, 2014, **4**, 1753-1763.
- 20 8. T. Xie, L. Shi, J. Zhang and D. Zhang, *Chem. Commun.*, 2014, **50**, 7250-7253.
- 21 9. H. Balcar and J. Čejka, *Coord. Chem. Rev.*, 2013, **257**, 3107-3124.
- 22 10. T. Ookoshi and M. Onaka, *Chem. Commun.*, 1998, 2399-2400.
- 23 11. L.-F. Chen, J.-C. Hu, Y.-D. Wang, K. Zhu, R. Richards, W.-M. Yang, Z.-C. Liu and W. Xu, *Mater.*  
24 *Lett.*, 2006, **60**, 3059-3062.
- 25 12. C. Lin, K. Tao, H. B. Yu, D. Y. Hua and S. H. Zhou, *Catal. Sci. Tech.*, 2014, **4**, 4010-4019.
- 26 13. T. I. Bhuiyan, P. Arudra, M. N. Akhtar, A. M. Aitani, R. H. Abudawoud, M. A. Al-Yami and S. S.  
27 Al-Khattaf, *Appl. Catal., A* 2013, **467**, 224-234.
- 28 14. W. Xu, C. Lin, H. Liu, H. Yu, K. Tao and S. Zhou, *RSC Adv.* 2015, **5**, 23981-23989.
- 29 15. X. Li, W. Zhang, S. Liu, L. Xu, X. Han and X. Bao, *J. Catal.*, 2007, **250**, 55-66.
- 30 16. D. P. Debecker, M. Stoyanova, U. Rodemerck, F. Colbeau-Justin, C. Boissere, A. Chaumonnot, A.  
31 Bonduelle and C. Sanchez, *Appl. Catal. A*, 2014, **470**, 458-466.
- 32 17. A. Tarasov, L. Kustov, V. Isaeva, A. Kalenchuk, I. Mishin, G. Kapustin and V. Bogdan, *Kinet.*  
33 *Catal.*, 2011, **52**, 273-276.
- 34 18. D. P. Debecker, M. Stoyanova, F. Colbeau - Justin, U. Rodemerck, C. Boissière, E. M. Gaigneaux

- 1 and C. Sanchez, *Angew. Chem. Int. Ed.* , 2012, **51**, 2129-2131.
- 2 19. J. Handzlik, J. Ogonowski, J. Stoch, M. Mikołajczyk and P. Michorczyk, *Appl. Catal. A* 2006, **312**,
- 3 213-219.
- 4 20. A. Ramanathan, B. Subramaniam, D. Badloe, U. Hanefeld and R. Maheswari, *J. Porous Mater.* ,
- 5 2012, **19**, 961-968.
- 6 21. Y. H. Guo, C. Xia and B. S. Liu, *Chem. Eng. J.* , 2014, **237**, 421-429.
- 7 22. B. Hu, H. Liu, K. Tao, C. Xiong and S. Zhou, *J. Phys. Chem. C*, 2013, **117**, 26385-26395.
- 8 23. B. Hu, C. R. Xiong, K. Tao and S. H. Zhou, *J. Porous Mater.* , 2015, **22**, 613-620.
- 9 24. V. V. Balasubramanian, P. Srinivasu, C. Anand, R. R. Pal, K. Ariga, S. Velmathi, S. Alam and A.
- 10 Vinu, *Microporous Mesoporous Mater.* , 2008, **114**, 303-311.
- 11 25. A. Ungureanu, B. Dragoi, V. Hulea, T. Cacciaguerra, D. Meloni, V. Solinas and E. Dumitriu,
- 12 *Microporous Mesoporous Mater.* , 2012, **163**, 51-64.
- 13 26. G. Karthikeyan and A. Pandurangan, *J. Mol. Catal.* , 2012, **361-362**, 58-67.
- 14 27. A. Prabhu, L. Kumaresan, M. Palanichamy and V. Murugesan, *Appl. Catal. A* 2009, **360**, 59-65.
- 15 28. H. Shankar, G. Rajasudha, A. Karthikeyan, V. Narayanan and A. Stephen, *Nanotechnology*, 2008,
- 16 **19**, 315711.
- 17 29. F. Kleitz, F. Bérubé, R. Guillet-Nicolas, C.-M. Yang and M. Thommes, *J. Phys. Chem. C*, 2010, **114**,
- 18 9344-9355.
- 19 30. J.-C. Hu, Y.-D. Wang, L.-F. Chen, R. Richards, W.-M. Yang, Z.-C. Liu and W. Xu, *Microporous*
- 20 *Mesoporous Mater.* , 2006, **93**, 158-163.
- 21 31. A. Ramanathan, R. Maheswari, B. P. Grady, D. S. Moore, D. H. Barich and B. Subramaniam,
- 22 *Microporous Mesoporous Mater.* , 2013, **175**, 43-49.
- 23 32. S. Doniach and M. Sunjic, *J. Phys. C: Solid State Phys.* , 1970, **3**, 285.
- 24 33. X.-L. Yang, W.-L. Dai, R. Gao and K. Fan, *J. Catal.* , 2007, **249**, 278-288.
- 25 34. M. Cortés-Jácome, C. Angeles-Chavez, E. Lopez-Salinas, J. Navarrete, P. Toribio and J. Toledo,
- 26 *Appl. Catal. A* 2007, **318**, 178-189.
- 27 35. M. Occhiuzzi, D. Cordischi, D. Gazzoli, M. Valigi and P. C. Heydorn, *Appl. Catal. A* 2004, **269**,
- 28 169-177.
- 29 36. L. Xu, C. Wang and J. Guan, *J. Solid State Chem.* , 2014, **213**, 250-255.
- 30 37. E. L. Lee and I. E. Wachs, *The J. Phys. Chem. C*, 2008, **112**, 6487-6498.
- 31 38. F. Figueras, J. Palomeque, S. Loridant, C. Fèche, N. Essayem and G. Gelbard, *J. Catal.* , 2004, **226**,
- 32 25-31.
- 33 39. J. L. Herisson and Y. Chauvin, *Makromol. Chem.*, 1971, **141**, 161-&.
- 34 40. R. H. Grubbs, P. L. Burk and D. D. Carr, *J. Am. Chem. Soc.* 1975, **97**, 3265-3267.
- 35 41. S. Meijers, L. Gielgens and V. Ponc, *J. Catal.* , 1995, **156**, 147-153.

36

37



W-Al-KIT-6 (Si/Al=10) with high dispersion of active W species and moderate acidity, shows highest activity and selectivity to propene.